

Plasma Surface Interactions (PSI): Improved PMI models for Plasma Edge codes and SOL Impurity Transport

J. Canik^(a), V. Chan^(b), D. Curreli^(c), R. Ding^(b), A. Laso^(a), P. Snyder^(b), X. Tang^(d),
B. Wirth^(e), T. Younkin^(e) and the PSI-SciDAC team

(a) Oak Ridge National Laboratory, (b) General Atomics, San Diego, (c) University of Illinois at Urbana Champaign, (d) Los Alamos National Laboratory, (e) University of Tennessee Knoxville

Improved PMI Models in SOLPS (ORNL, LANL)

Two improvements to the PMI models within SOLPS have been explored:

1. Sheath Heat Transmission Coefficients

- Determine relationship between heat flux onto surface and temperature of plasma in contact
- Based on analytic models, supported by some kinetic simulation
- Sheath heat transmission is set as boundary condition on fluid eqns
- Bohm condition on parallel ion flow speed

- Ambipolar flux to wall gives potential
- Kinetic consideration give sheath heat transmission factors γ_e, γ_i

$$j_x = en \left(b_x c_x - b_x \frac{1}{\sqrt{2\pi}} \frac{T_e}{m_e} \exp\left(-\frac{e\Phi}{T_e}\right) (1 - \gamma_e) \right)$$

$$\tilde{q}_{ex} = b_x \frac{n}{\sqrt{2\pi}} \frac{T_e}{m_e} \exp\left(-\frac{e\Phi}{T_e}\right) (1 - \gamma_e) \left(T_e \frac{1 + \gamma_e}{1 - \gamma_e} + e\Phi \right)$$

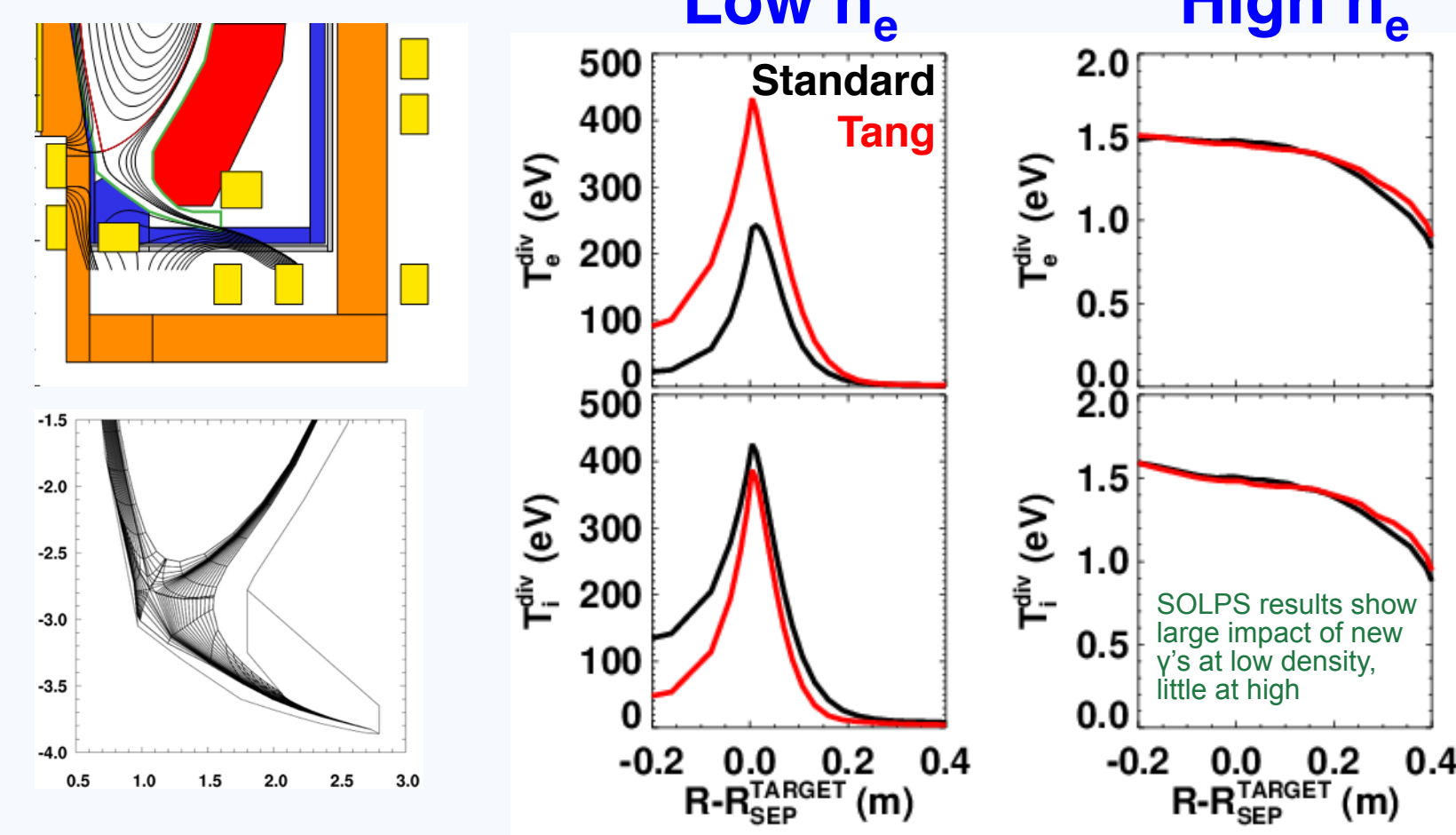
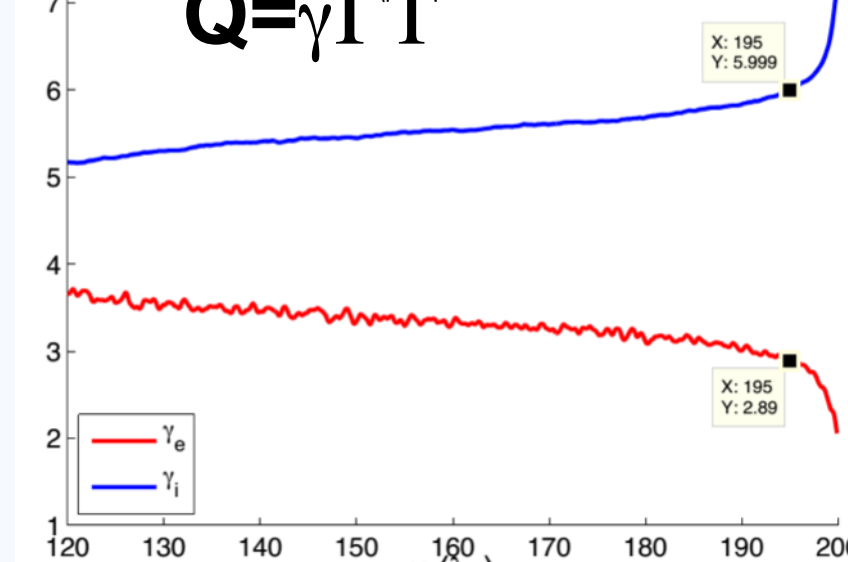
$$\tilde{q}_{ix} = \frac{3}{2} n T_i c_x b_x$$

ST-FNSF 'Super-X' simulated with new sheath heat transmission coefficients

- Runs based on design study of ST-FNSF
 - Menard, SOFE '13 and Canik, IEEE TPS '14; P_{SOL}=50MW, λ_D~1-2mm
 - Pure deuterium plasmas simulated, plus radiation assuming N fraction of 2%
- Novel divertor described in P.M. Valanju et al, PoP 2009
 - Characteristic feature: radially extended outer divertor
 - Larger wetted area, longer connection length

Sheath Transmission factor	Conventional	Tang sim
γ_e	5	3.3-4.5
γ_i	1.5-2.5	5.4-5.9

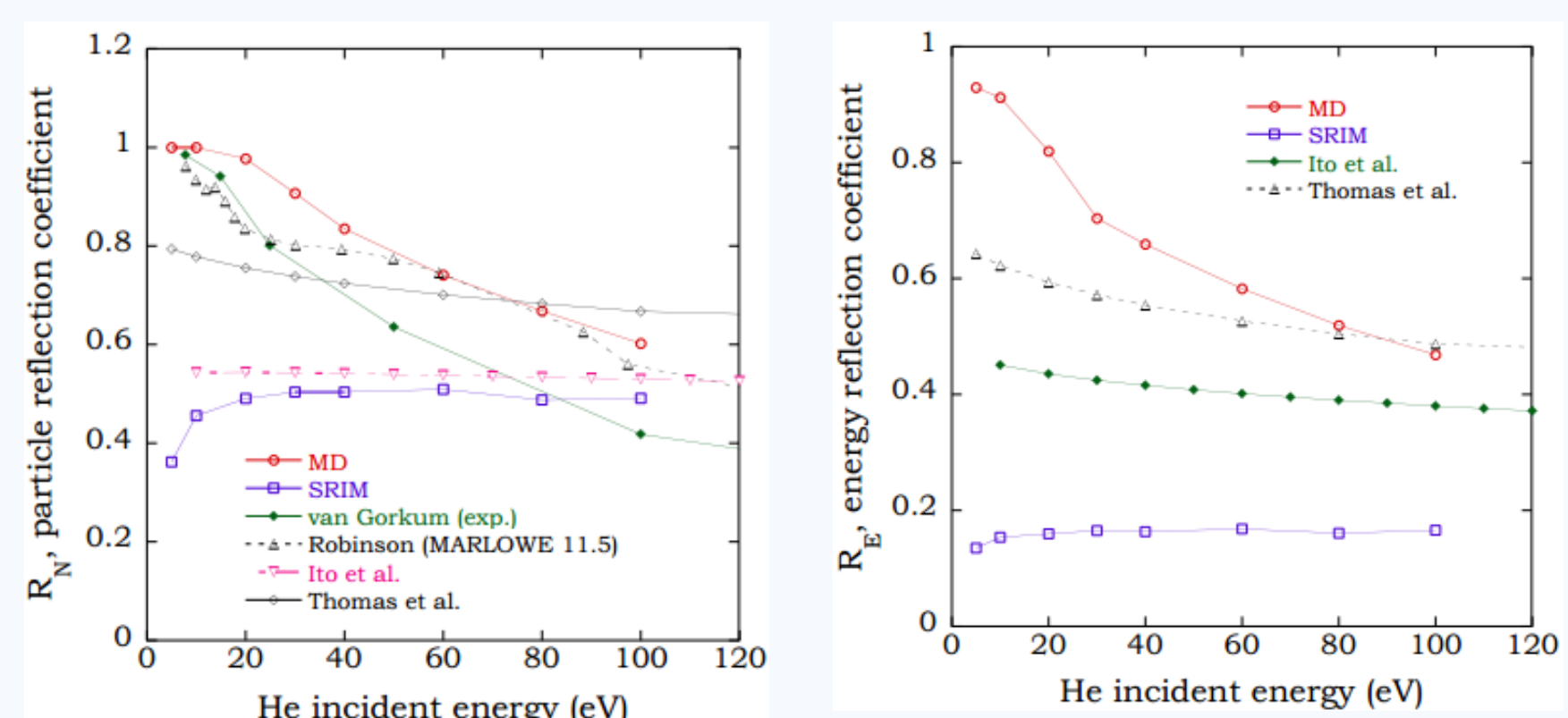
Variations are mainly due to collisionality
(1) γ_i has very little variation w.r.t collisionality
(2) γ_e does have significant variation w.r.t collisionality



Xian-Zhu Tang and Zehua Guo, Sheath energy transmission in a collisional plasma with collisionless sheath, Submitted

2. High Reflection Coefficients

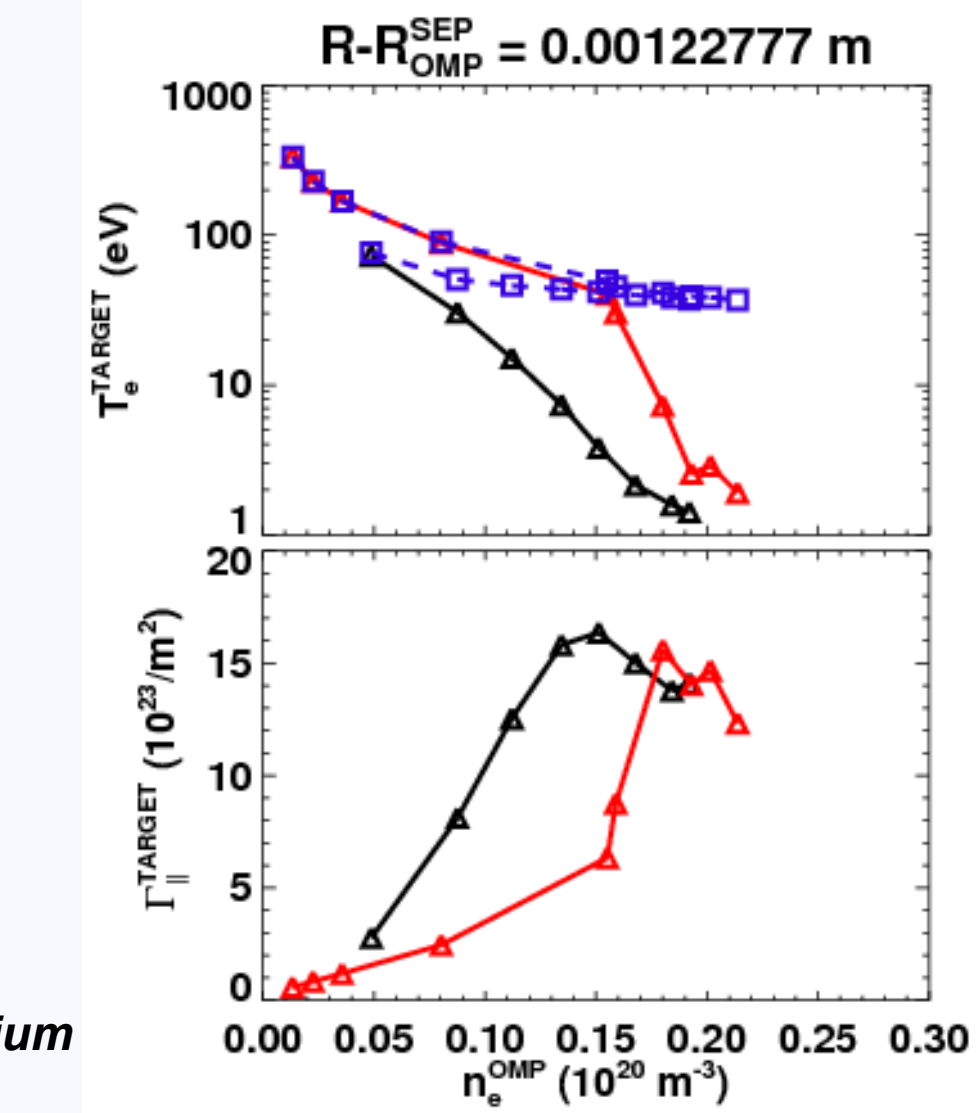
- Typically most (75%) incident ions are adsorbed onto surface, desorb as atoms/molecules at wall temperature
- Some plasma/material compositions lead to very high fractions of incident ions reflected as fast neutrals without loss of energy
- LANL MD sims show high particle and energy reflection for He->W
- Nothing changes in terms of plasma boundary conditions (wall is still perfect sink of ions/electrons)
- But: now power carried by ions comes back as fast neutrals
- Likely: neutral CX will heat plasma equal to ion power loss, so Te has to increase until electrons carry all the input power to the wall



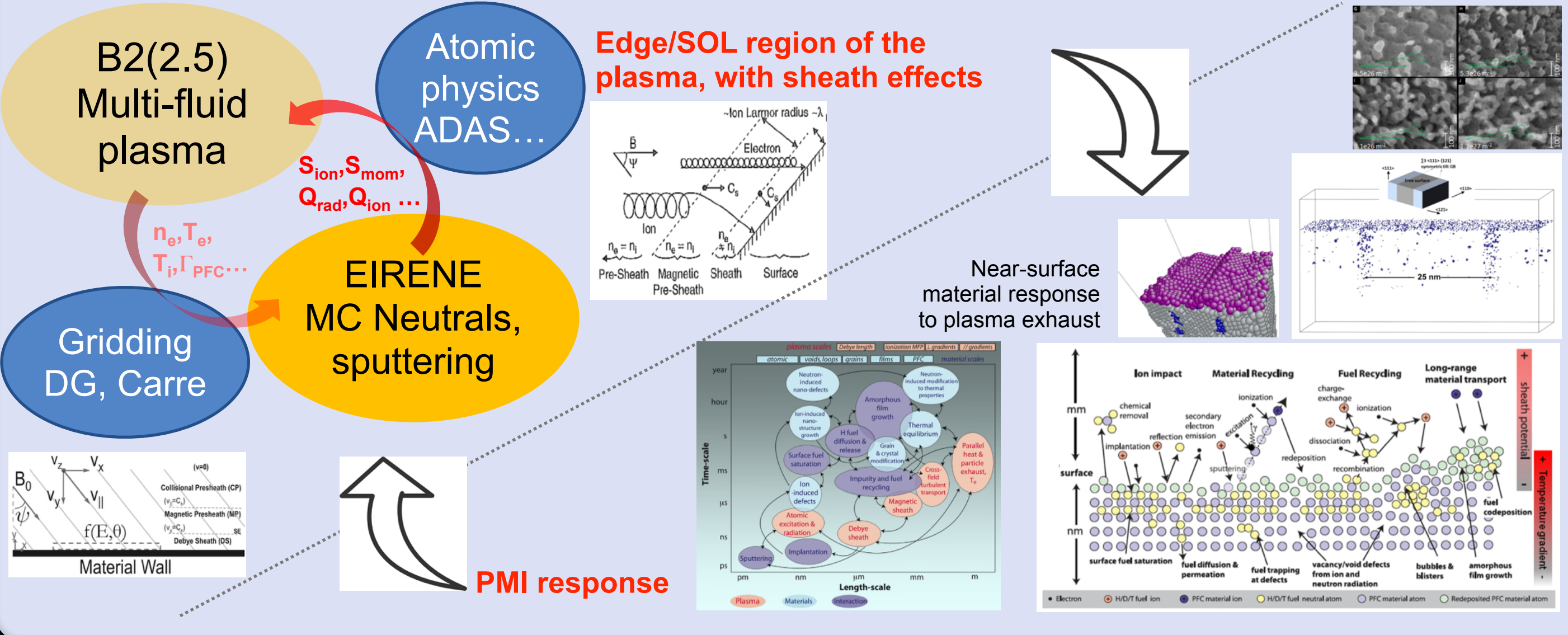
V. Borovikov, A.F. Voter, X. Tang, Reflection and implantation of low energy helium with tungsten surfaces, J. Nucl. Mat. 447, 254 (2014)

DIII-D case study

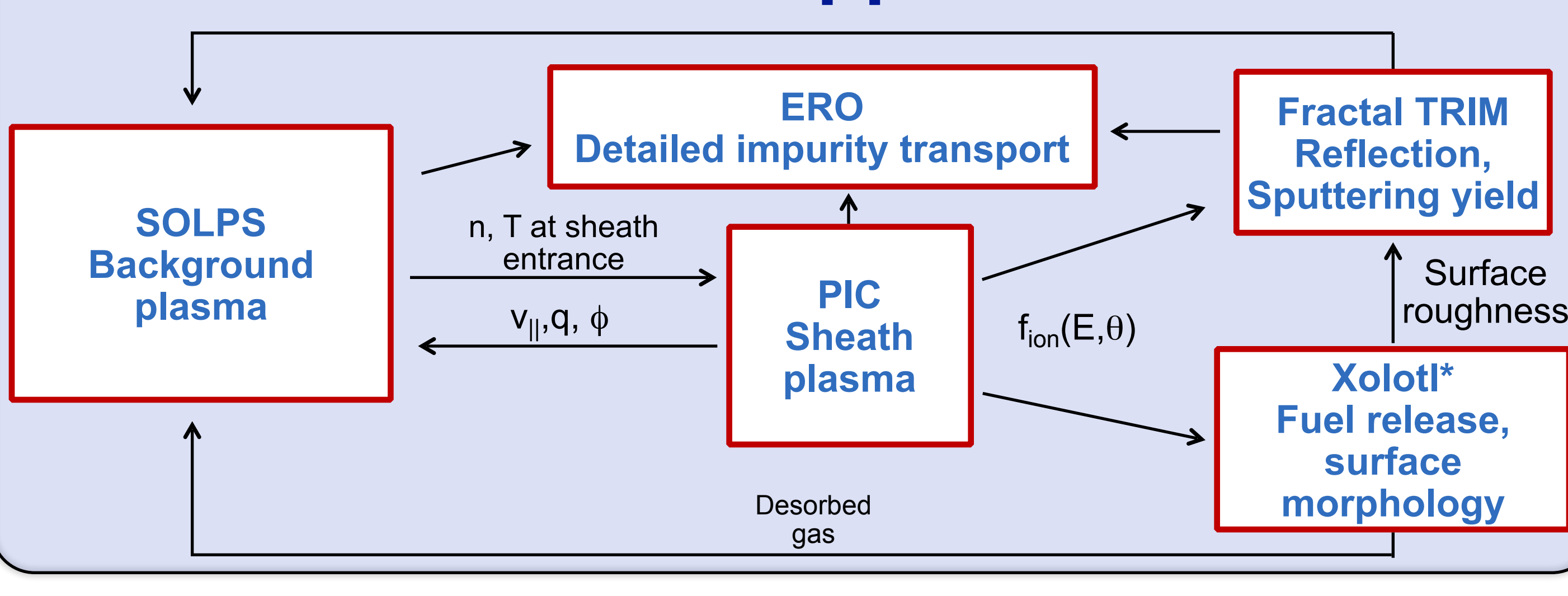
- Higher upstream density required for low T, detachment with high reflection
- High reflection overall is much stronger effect than seen with altered sheath heat transmission
- Significantly hotter SOL observed
- Access to detached conditions requires higher density
 - By ~20% for both low Te and particle flux rollover



In order to address key scientific PMI issues, an integrated Edge-PMI approach is required



Current Approach

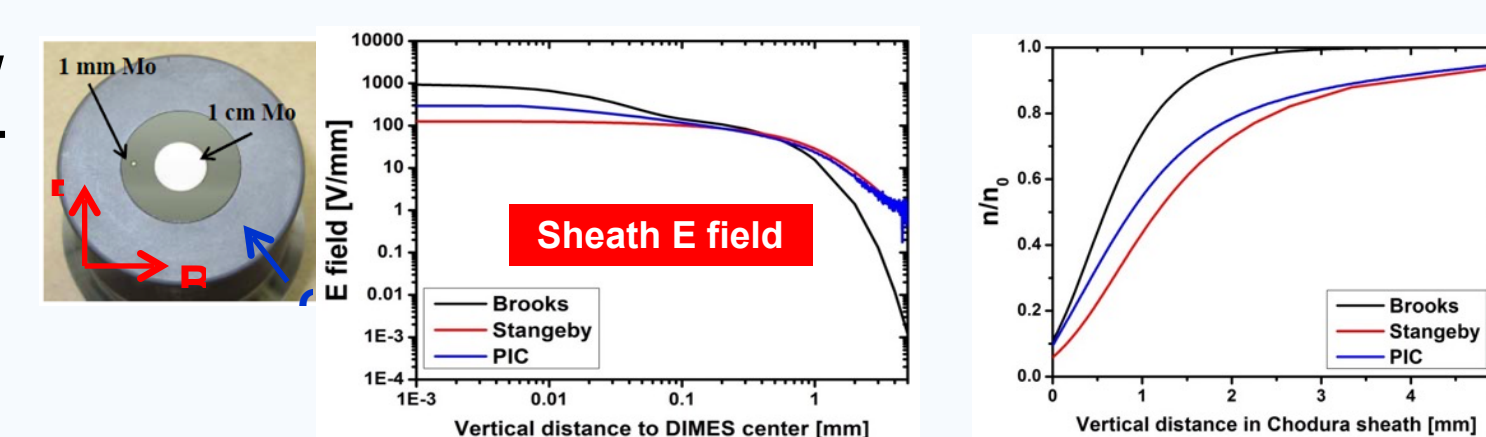


ERO Monte Carlo modeling of gross/net erosion of DIII-D DIMES (GA) and antenna-connected Be limiters at JET (ORNL)

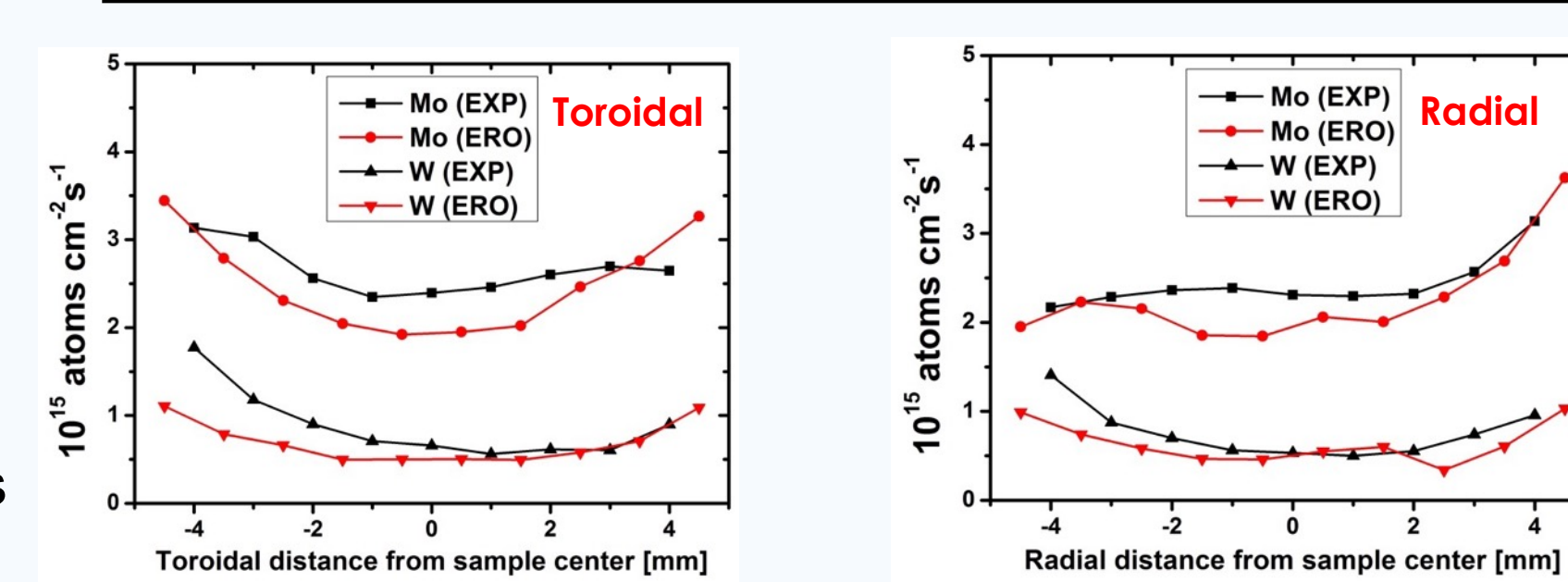
1. Gross and net erosion of Mo and W in DIII-D DIMES experiments (GA)

- DIMES: 1 cm sample for net erosion and 1 mm sample for gross erosion, made of thin Mo/W film on Si substrate
- Inputs: OEDGE background plasma providing n_e, T_e, E_{||}; B_t = 2.25 T, pitch angle: 1.5°
- C³⁺, Roth formula for chemical erosion yield; homogeneous material mixing model
- Erosion & deposition measured via RBS
- Similar redeposition ratios obtained from ERO simulations using 3 sheath models (Brooks, Stangeby, PIC)
- The redeposition ratio from ERO simulation is dominated by the electric field and plasma density within the magnetic pre-sheath
- Density decay within magnetic pre-sheath leads to lower redeposition ratio due to larger Mo ionization length
- Net erosion rate and redeposition ratio of both Mo and W are well reproduced by ERO modeling

R. Ding et al., Simulation of gross and net erosion of high-Z materials in the DIII-D divertor, To be subm.



	Mo		W	
	EXP	ERO	EXP	ERO
Net erosion rate (nm/s)	0.42	0.43	0.18	0.14
Redeposition ratio (1cm)	44 % (46%)	39 %	63% (67%)	67%
Redeposition ratio (1mm)	N/A	4 %	N/A	14%

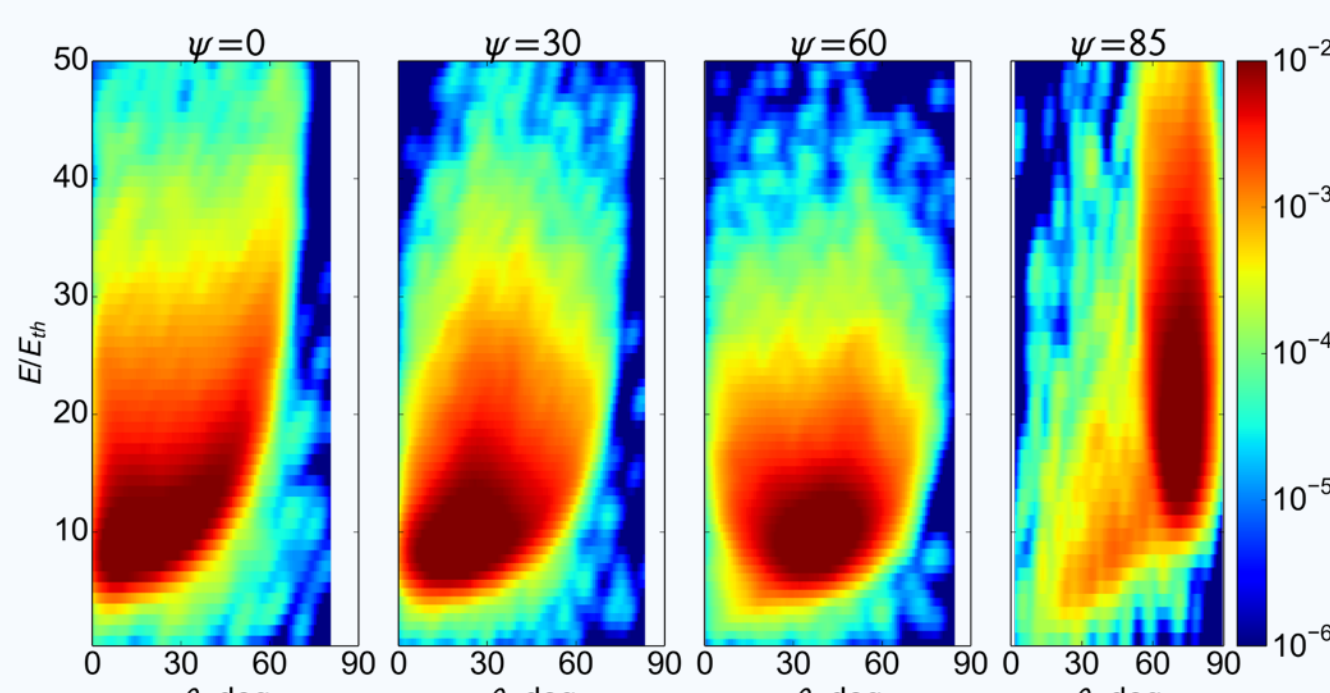


	1 cm sample		1 mm sample	
	EXP	ERO	EXP	ERO
ERO (Brooks, no re-variation)	65%	65%	18%	18%
ERO (Stangeby, no re-variation)	64%	64%	18%	18%
ERO (PIC, no re-variation)	63%	63%	18%	18%
ERO (Brooks, with re-variation)	39%	39%	4%	4%
ERO (Stangeby, with re-variation)	38%	38%	3%	3%
ERO (PIC, with re-variation)	36%	36%	3%	3%

PIC Plasma Sheath and Fractal TRIDYN (UIUC)

1. Ion Energy-Angle Distribution in Magnetized Plasma Sheath

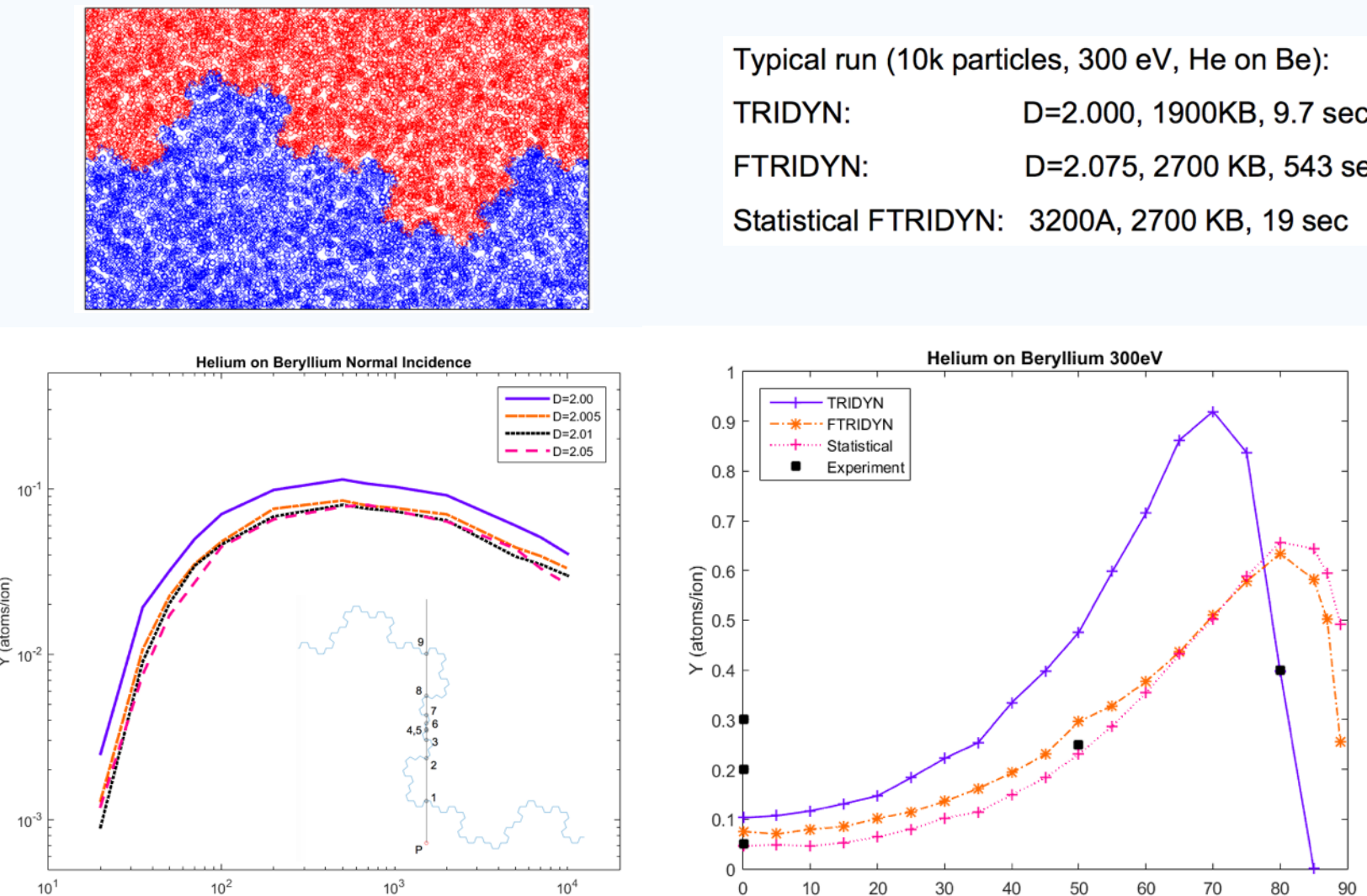
- Plasma Sheath: establishes the link between "Edge" and "Wall"
- UIUC full-f 6D sheath PIC code used to analyze the near-wall ion kinetics
- PIC Characterization of the Ion Energy-Angle Distributions (IEAD) in oblique magnetic fields
- IEAD are a necessary input to material & PMI models



R. Khaziev, D. Curreli, Ion energy-angle distribution functions at the plasma-material interface in oblique magnetic fields, Phys. Plasmas 22, 043503 (2015)

2. Development of Fractal-TRIDYN

- Finite surface roughness and surface morphology affect the sputtering processes and the impurity release
- Improved Fractal-TRIDYN algorithm decreases computational complexity from O(n²) to O(n), with x20 gain in computational speed
- In addition, a new approach based on a statistical description of surface morphology has been developed
- New statistical algorithm reproduces same results of Fractal-TRIDYN
- Statistical algorithm is x28 faster than the improved O(n) fractal algorithm



J. Drobny, D. Curreli, D. Ruzic, Improved Fractal Algorithm for the Treatment of Surface Roughness in Binary-Collision Approximation Codes. To be subm.
J. Drobny, D. Curreli, A Statistical Treatment of Surface Roughness for Binary-Collision Approximation Codes To be subm.

2. Estimates of RF-Induced Erosion at Antenna-Connected Beryllium Limiters in JET (ORNL)

- 3D Monte Carlo code ERO aiming to reproduce enhanced Be erosion due to RF antennas; no direct simulation of the RF-enhanced sheath, but introduced in ERO by applying and varying additional surface negative biasing, V = 0-300 eV

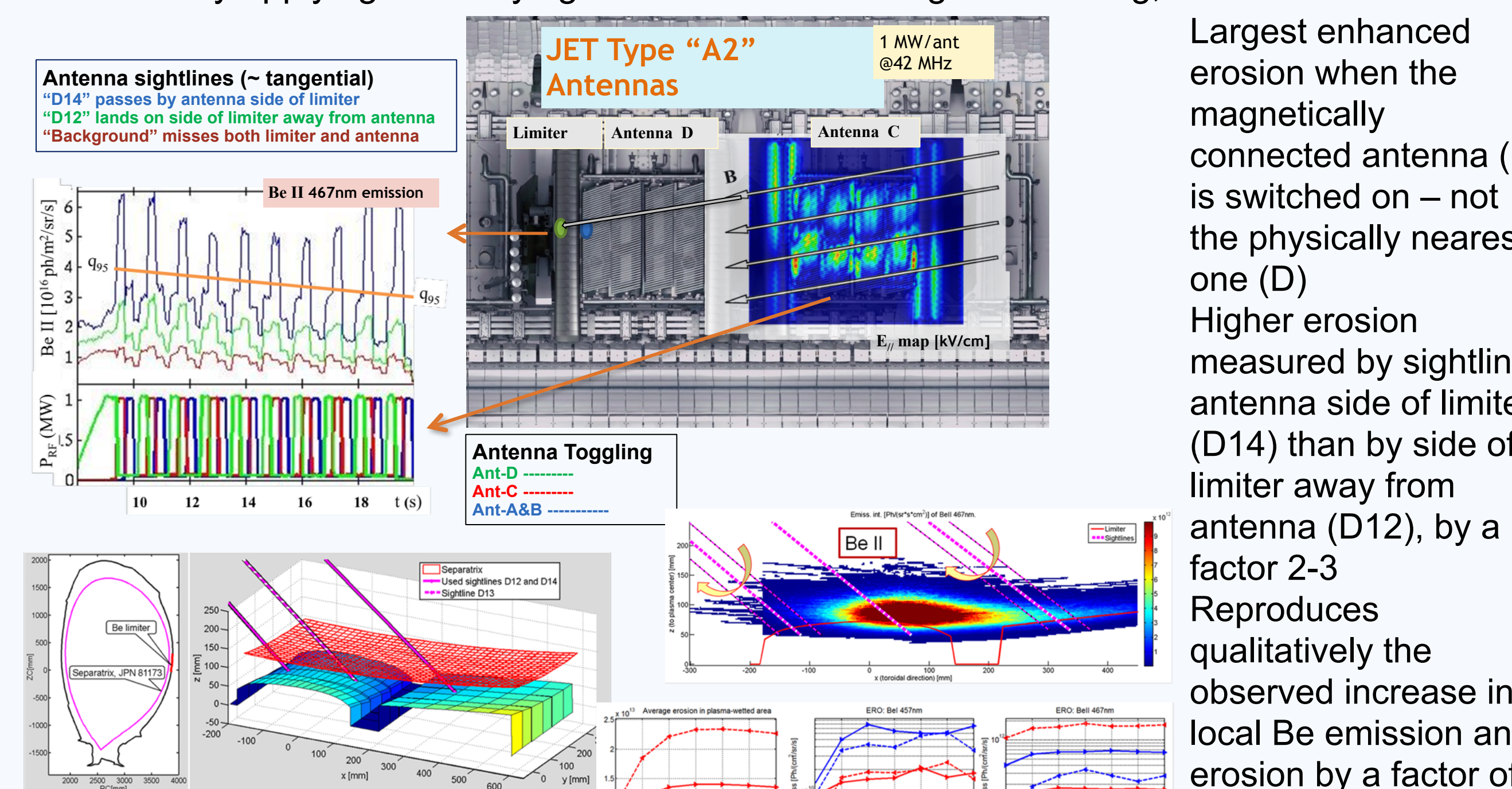


Fig. 3. ERO code grid wrt relevant antenna/limiter surfaces and sightline

C.C. Klepper, D. Borodin, A. Laso, et al. Estimates of RF-Induced Erosion at Antenna-Connected Beryllium Plasma-Facing Components in JET, PFMC-15, Submitted

Largest enhanced erosion when the magnetically connected antenna (C) is switched on - not the physically nearest one (D)
Higher erosion measured by sightline antenna side of limiter (D14) than by side of limiter away from antenna (D12), by a factor 2-3
Reproduces qualitatively the observed increase in local Be emission and erosion by a factor of ~2-3 with RF biasing (from remote antenna)